Journal of Biomedical Optics

SPIEDigitalLibrary.org/jbo

Trapping and two-photon fluorescence excitation of microscopic objects using ultrafast single-fiber optical tweezers

Yogeshwar N. Mishra
Ninad Ingle
Samarendra K. Mohanty

SPIE

Trapping and two-photon fluorescence excitation of microscopic objects using ultrafast single-fiber optical tweezers

Yogeshwar N. Mishra,[a,b] Ninad Ingle,[a] and Samarendra K. Mohanty[a]
[a]University of Texas at Arlington, Department of Physics, Arlington, Texas 76019
[b]Centre of Excellence in Lasers and Optoelectronic Sciences, CUSAT, Cochin 682022, India

Abstract. Analysis of trapped microscopic objects using fluorescence and Raman spectroscopy is gaining considerable interest. We report on the development of single fiber ultrafast optical tweezers and its use in simultaneous two-photon fluorescence (TPF) excitation of trapped fluorescent microscopic objects. Using this method, trapping depth of a few centimeters was achieved inside a colloidal sample with TPF from the trapped particle being visible to the naked eye. Owing to the propagation distance of the Bessel-like beam emerging from the axicon-fiber tip, a relatively longer streak of fluorescence was observed along the microsphere length. The cone angle of the axicon was engineered so as to provide better trapping stability and high axial confinement of TPF. Trapping of the floating objects led to stable fluorescence emission intensity over a long period of time, suitable for spectroscopic measurements. Furthermore, the stability of the fiber optic trapping was confirmed by holding and maneuvering the fiber by hand so as to move the trapped fluorescent particle in three dimensions. Apart from miniaturization capability into lab-on-a-chip microfluidic devices, the proposed noninvasive microaxicon tipped optical fiber can be used in multifunctional mode for in-depth trapping, rotation, sorting, and ablation, as well as for two-photon fluorescence excitation of a motile sample. [DOI: 10.1117/1.3643340]

Keywords: optical tweezers; fiber optic tweezers; optical manipulation; two-photon fluorescence.

Paper 11271PR received Jun. 2, 2011; revised manuscript received Aug. 25, 2011; accepted for publication Aug. 26, 2011; published online Oct. 3, 2011.

1 Introduction

Single beam near-infrared (NIR) optical tweezers[1] provides unprecedented precision in investigating and manipulating microscopic objects, especially the living cells and molecules inside a sterile and closed environment. This allowed long-term fluorescence[2] and Raman[3] spectroscopic analysis of motile cells being immobilized by the tweezers without perturbing their natural environment. Though the large power density at the focused spot of a continuous wave (cw) laser beam is sufficient for excitation of fluorescence by two-photon excitation,[4,5] the use of a pulsed beam for multiphoton excitation[6] provides a stronger two-photon fluorescence (TPF) signal of the optically trapped sample.[7,8] A single NIR pulsed laser beam based[9] optical tweezers has been used to trap and excite TPF in the trapped microscopic objects. In spite of these technological advances, conventional optical tweezers-based trapping in three dimensions requires a high numerical aperture (NA) microscope objective so that axial gradient force is large enough to overcome the scattering and absorption forces. The low working distance of the high NA objective severely limits the depth at which the objects can be manipulated and analyzed. This has propelled the development of fiber optic-based optical trapping[10–14] and analysis. Though counterpropagating laser beams[10] from two single mode fibers with cleaved or lensed ends have been initially used to trap microscopic objects in three dimensions, it requires perfect alignment of the two fibers. Further, the effective size of the fiber-probe is limited by the bending radius of the fibers and therefore not suitable for in-depth applications. The single-beam fiber with spherical lens on the tip could only trap objects in two-dimensions.[11] This can be attributed to the fact that tight focusing of a beam from a single mode fiber using a spherical microlens is not free from aberrations which leads to smaller restoring force in axial direction. Even use of a taper or axicon[12] on a fiber tip for trapping required an additional counter-balancing force of nonoptical origin.

However, proper design and fabrication of micro-axicon on tip led to realization[13,14] of three-dimensional trapping using a single optical fiber. The three-dimensional (3D) cw trapping using a fiber axicon microlens was possible[13,14] due to nearly diffraction-limited focusing[15] and characteristic Bessel–Gauss beam profile emerging from the microaxicon tip fiber. For large tip cone angles, the scattering force of the output beam from the microaxicon single mode fiber on dielectric objects has been shown to be reduced as compared to the axial gradient force. Here, we report the development of femtosecond fiber optic tweezers for simultaneous in-depth trapping and two-photon excitation in fluorescent microscopic objects. Most notably, trapping depth of a few centimeters was achieved inside a colloidal sample with TPF from the trapped object being visible to the naked eye.

Address all correspondence to: Samarendra Mohanty, University of Texas at Arlington, Biophysics and Physiology Group, Department of Physics, 502 Yates Street, 108 Science Hall, Arlington, Texas 76019; Tel: 817-272-1177; Fax: 817-272-3637; E-mail: smohanty@uta.edu.

1083-3668/2011/16(10)/105003/8/$25.00 © 2011 SPIE

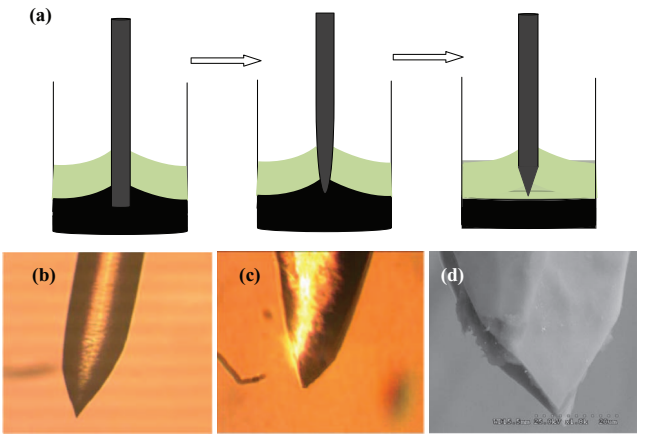

Fig. 1 (a) Time-lapse schematic of the chemical etching process. (b) Microscopic image of the axicon tip fabricated using single-stage self-terminating etching process. (c) Microaxicon tip fabricated using two-step etching process. (d) SEM micrograph of a microaxicon tip.

2 Materials and Methods

2.1 *Fabrication of Microaxicon Fiber Tip*

Single mode optical fiber appropriate for 980 nm was used for preparing the axicon-tip fiber. One end of the mechanically cleaved bare single mode fiber was dipped into 50% hydrofluoric (HF) acid containing a protective layer (e.g., Toluene) at the top [Fig. 1(a)]. The tip formation takes place at the interface of the etching liquid and the protecting overlayer. As described by Hoffmann et al.[16] the cone angle of the fiber tip is determined by the contact angle of HF with the fiber. The etching process is self-terminating and the cone angle is influenced by the liquid used as the top protection layer. Figure 1(b) shows a microscopic image of an axicon tip, prepared using a single stage chemical etching process. For fabrication of a large cone angle tip, the two-step etching technique[17] was employed. After the first selective chemical etching step, the tapered region has a small cone angle. The second selective etching resulted in large cone angle axicon tip [Fig. 1(c)]. Figure 1(d) shows the SEM image of such a tip.

2.2 *Experimental Setup and Schematic of Fiber-Optic Tweezing and Two-Photon Excitation*

The schematic experimental setup for fiber optic tweezers and two-photon excitation is shown in Fig. 2(a). The output of the Ti:Sapphire laser (Maitai HP, Newport Spectra-Physics, Inc.) was expanded (BE) and coupled into the cleaved end of the axicon-tip single mode optical fiber using a 10× microscope objective (O). The microaxicon tip end of the fiber was held by an XYZ mechanical manipulator (or hand) and inserted into the cuvette (C). A side-viewing 10× microscope objective was used to image the microaxicon tip, trapped microspheres, and the two-photon fluorescence onto a video camera. In some cases,

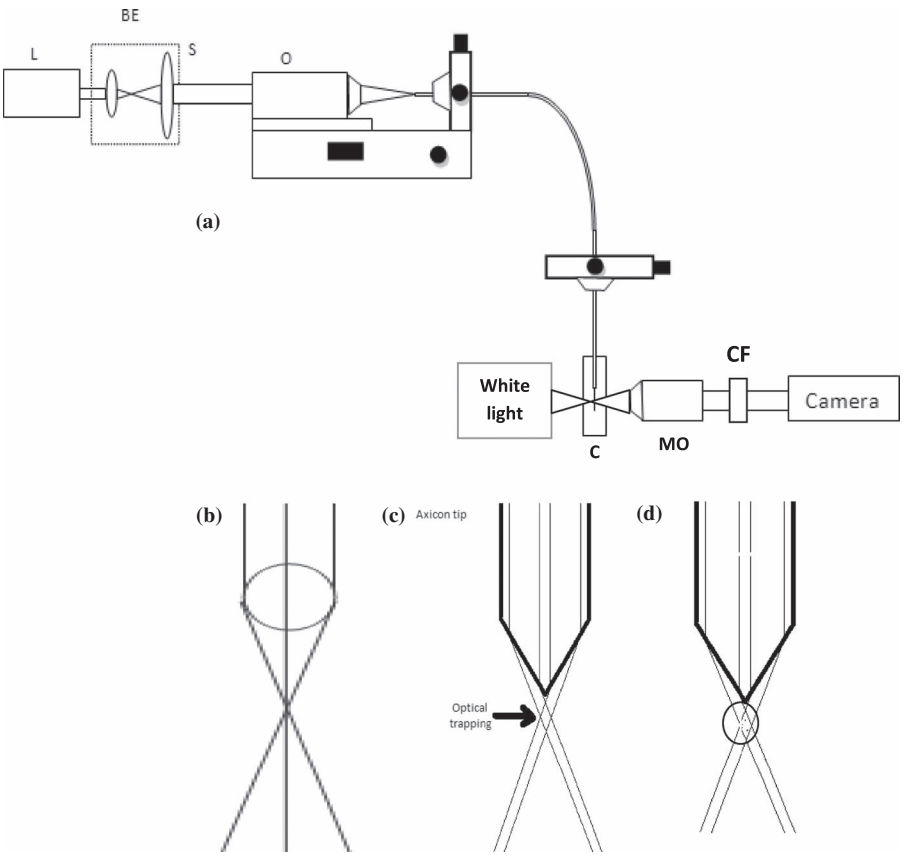

Fig. 2 (a) The schematic experimental setup for fiber optic tweezers and two-photon excitation. L: Ti: Sapphire laser; BE: beam expander; S: Shutter; O: 10× microscope objective; C: cuvette; MO: microscope objective; CF: cut-off filter. Ray propagation for a microlens (b) versus microaxicon (c). (d) Schematic of two-photon fluorescence excitation in the trapped object along the optic axis by the Bessel–Gauss beam.

the two-photon fluorescence was observed by the naked eye by using a laser-safety eye glass or using a 100× microscope objective. The suspension of fluorescent polystyrene beads, dispersed in distilled water, was placed in the cuvette (C), and transilluminated using a white light source. An infrared cut-off filter was used to block the NIR laser beam reaching the CCD. The images of trapping and two photon excitation (TPE) of objects were digitized using a frame grabber and computer. The image analysis was done using Image J software.

3 Beam Propagation for Two-Photon Excitation and 3D Trapping

3.1 *Measurement of Beam Profile Through Microaxicon*

An axicon is a specialized type of lens having a conical surface, which can be used to turn a Gaussian beam into a Bessel beam, with greatly reduced diffraction. Recent studies have shown[15] that conical optics can focus better than spherical ones with the smallest optical confinement zones. Figures 2(b) and 2(c) show a schematic of ray propagation through a microlens versus microaxicon. No central ray along the optical axis, in the case of a microaxicon [Fig. 2(c)], ensures the least scattering force as compared to axial gradient force. Due to this special nature of the Bessel − Gauss beam (having a small high-intensity region along the *Z*-direction), relatively low NA (or less diverging beam) can achieve single beam optical tweezers as compared to traditional Gaussian beam optical tweezers. The two-photon excitation inside the trapped object occurs along the optic axis throughout the propagation distance [Fig. 2(d)], which depends on the tip cone angle of the microaxicon.

For different cone angle tips, the transverse beam profiles and propagation distance were measured by using a microscope objective, translated over a 20 μm range with a resolution of 1 μm. The measured beam profiles at different distances from the tip showed truncated Bessel-like beam profiles with few concentric rings. For a very small cone angle tip, the rays coming out from radially opposite locations of the tip do not intersect in contrast to the situation shown in Fig. 2(c). Further, transmittance of the beam through the smaller microaxicon cone angle tip (<30 deg) fiber was found to decrease substantially, which can be attributed to an increase in total internal reflection at the fiber tip. Though these tips might be well-suited for near-field scanning microscope applications, two-photon excitation, and 3D-trapping requires higher transmittance and the highest intensity spot away from the tip. For a very large cone angle (>90 deg) tip, though transmittance is high, the propagation distance of the emanating laser beam profile is too large to generate sufficient axial gradient force for efficient 3D trapping. Therefore, for optimal two-photon fluorescence excitation and 3D trapping, anintermediate cone angle, i.e., between 40 to 60 deg, was used.

3.2 *Simulation of Beam Profile Through Microaxicon*

Truncated-Bessel (or Bessel Gauss) beams, having different propagation characteristics, can be generated by engineering the axicon microstructure on the tip of the single mode fiber. For simulation of a beam profile emanating from the axicon microstructure, let us start with the fundamental mode of the fiber, $E_{\text{fund}} \approx \exp(-(X^2+Y^2)/\omega^2)$ where ω is the mode field size. The electric field propagating from the tip at any observation point (x_0,y_0) can be described[18] as:

$$E(x_o, y_o) = \frac{\exp(ikz)}{i\lambda z} \times \exp\left[i\frac{k}{2z}\left(x_o^2+y_o^2\right)\right]\int_{-\infty}^{\infty}\int_{-\infty}^{\infty}\left\{E(x_1, y_1) \times \exp\left[i\frac{k}{2z}\left(x_1^2+y_1^2\right)\right]\right\} \times \exp\left[-i\frac{2\pi}{\lambda z}(x_o x_1 + y_o y_1)\right]dx_1 dy_1, \quad (1)$$

where $E\ (x_1,y_1)$ is the field at the point (x_1,y_1) on the base of the microaxicon, which can be calculated usingE_{fund} and accounting for the phase acquired along the axicon-tip region. For axicon base radius (r) of 3 μm, height of axicon (T) = 5.4 μm, and half tip cone angle (θ) of 29 deg [Fig. 3(a)], the transverse beam profiles at different axial distances from the tip was simulated for laser beam wavelength of 900 nm. Figure 3(b) shows a typical mode profile of the NIR beam transmitted through the axicon tip fiber calculated at a distance of 10 μm from the axicon tip. The fewer rings in Fig. 3(b) are indicative of the truncated nature of the Bessel beam obtained when a microaxicon is illuminated by a Gaussian beam of very small size (core diameter of fiber ~ 6 μm). The refractive index of axicon and water (as the surrounding medium) was taken as 1.5 and 1.33, respectively, for these calculations. Since the beam profile measurements were done in air as surrounding medium, the experimental measurements were not in exact agreement with these theoretical simulations. The simulations showed the beam waist is smallest at a distance of ~5 μm from the tip of the axicon for $\theta = 29$ deg. Therefore, the two-photon fluorescence intensity excited by the beam is expected to be highest at this axial distance for these microaxicon parameters. Further, the propagation distance was found to be ~6 μm.

3.3 *Radiation Forces Due to Axicon Tip Fiber Tweezers in Rayleigh Regime*

The optical trapping forces on the Rayleigh particles[19] due to the beam emanating from the microaxicon fiber tip can be calculated using the transverse beam profiles [Fig. 3(b)] obtained at different axial distances. Considering a dielectric sphere (radius $a = 50$ nm, dielectric constant ε_1) in a medium (dielectric constant ε_2; magnetic permeability μ_2) being illuminated by a linearly polarized (parallel to the x axis) z-propagating beam from the microaxicon. The Rayleigh particle in the instantaneous electric field $\vec{E}(r,t)$acts as a point dipole, whose dipole moment (in MKS units) is given by

$$\vec{p}(r,t) = 4\pi\varepsilon_2 a^3\left(\frac{\varepsilon_1-\varepsilon_2}{\varepsilon_1+2\varepsilon_2}\right)\vec{E}(r,t) = 4\pi\varepsilon_0 n_2^2 a^3\left(\frac{m^2-1}{m^2+2}\right)\vec{E}(r,t), \quad (2)$$

where $m = n_1/n_2$ (in our case, 1.59/1.33) is the relative refractive index of the particle. The radiation pressure force exerted on the

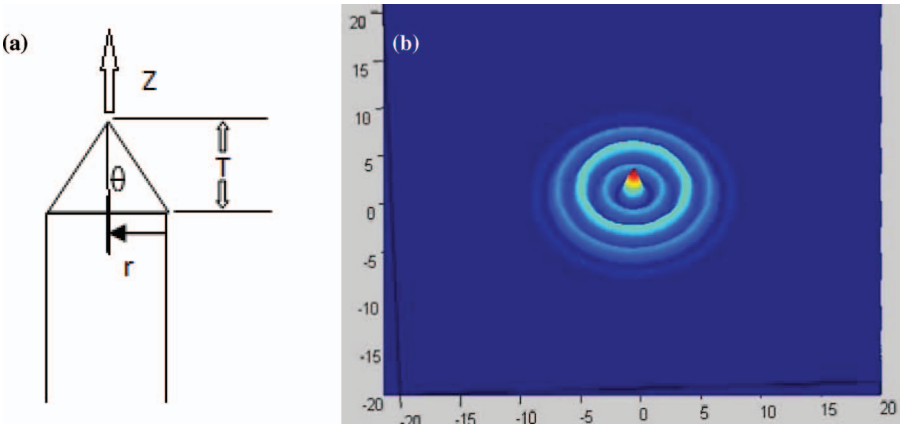

Fig. 3 (a) Nomenclature for the microaxicon. (b) Simulated beam profile of the laser beam ($\lambda = 900$ nm) transmitted through the axicon tip ($T = 5.4$ μm, $r = 3$ μm, $\theta = 29$ deg) at distance of ~10 μm. The scale in X and Y axis is in micrometers.

particle in the Rayleigh regime has two components. One of these force components is a so-called scattering force, given by

$$F_{sc}(r) = \hat{z} n_2 I(r) \frac{C_{sc}}{c},$$

where

$$C_{sc} = \frac{8}{3}\pi (ka)^4 a^2 \left(\frac{m^2-1}{m^2+2}\right)^2. \quad (3)$$

The other component is a gradient force due to the Lorentz force acting on the dipole induced by the electromagnetic field. By using the electric dipole moment of Eq. (2) as an electrostatics analogue of the electromagnetic wave, the instantaneous gradient force is defined by

$$\vec{F}_{\text{grad}}(r,t) = [\vec{p}(r,t).\nabla]\vec{E}(r,t)$$
$$= 4\pi\varepsilon_0 n_2^2 a^3 \left(\frac{m^2-1}{m^2+2}\right)\frac{1}{2}\vec{E}^2(r,t). \quad (4)$$

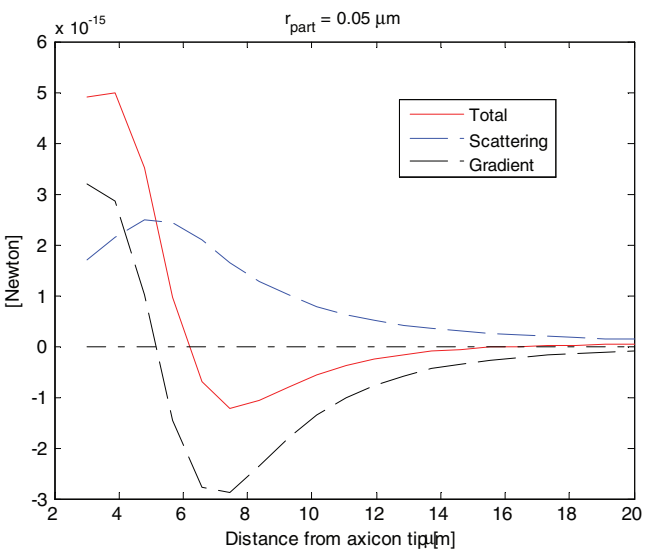

Fig. 4 Plot of radiation forces on a 50 nm polystyrene particle due to trapping beam power of 100 mW. Arrow points to stable axial trapping position.

The gradient force which the particle experiences in a steady state is the time-average version of Eq. (4) and is given by

$$\vec{F}_{\text{grad}}(r) = \frac{2\pi n_2 a^3}{c}\left(\frac{m^2-1}{m^2+2}\right)\nabla I(r). \quad (5)$$

By substituting the obtained mode profiles [Fig. 3(b)] in Eqs. (3) and (5), respectively, the scattering and gradient forces were obtained (Fig. 4).

Figure 4 shows the calculated scattering and axial gradient force as well as the total force along an axial direction on a polystyrene particle ($n = 1.59$) of radius 50 nm due to a laser beam power of 100 mW propagating through the axicon tip ($T = 5.4$ μm, $r = 3$ μm, $\theta = 29$ deg). From Fig. 4, it is clear that the particle will be stably trapped along the axial direction (in addition to transverse directions by gradient force) at a distance of ~ 6 μm (arrow marked) from the tip of the axicon. This is consistent with the fact that the beam width is minimal at a distance of ~5 μm from the tip of the axicon [Fig. 3(b)] and the stable axial trapping position is shifted away from the axicon tip due to the scattering force. This stable axial trapping position and the magnitude of the axial trapping force were found to depend on the cone angle of the axicon as well as its refractive index and size of the particle. Therefore, the particle is expected to be trapped in this axial region. This stable trapping point and the magnitude of the trapping force were found to depend on the cone angle as well as refractive index of the axicon and size of the particle.

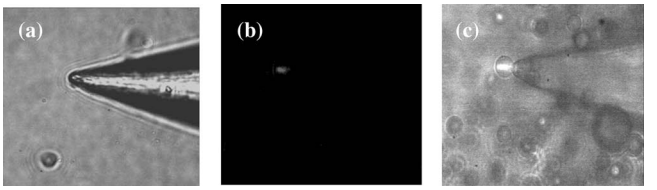

Fig. 5 (a) Bright field image of an axicon tip with $\theta = 20$ deg. (b) Two-photon excitation in the trapped bead. (c) Bright field image also showing the two-photon fluorescence from the bead.

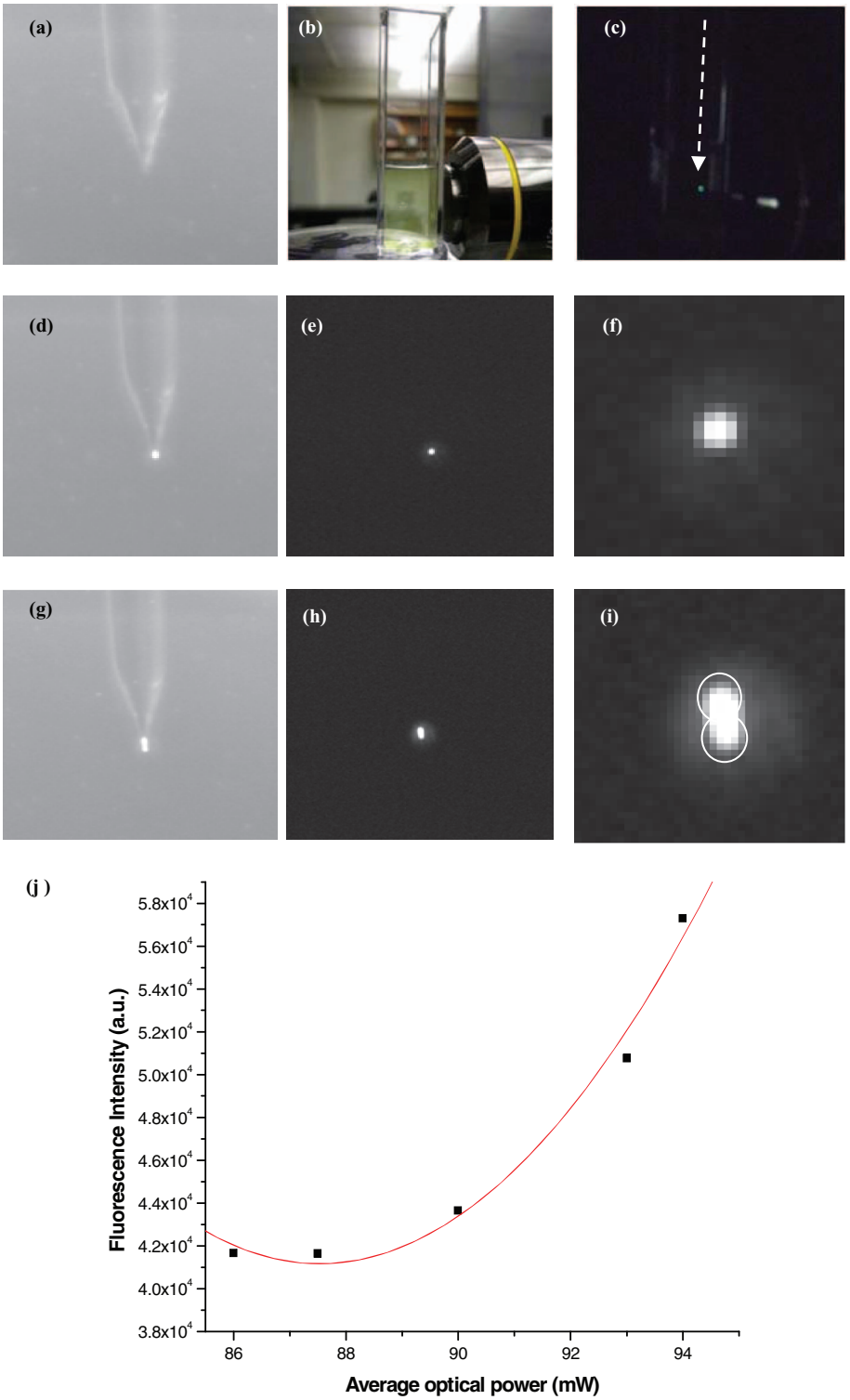

Fig. 6 (a) Bright field images of the axicon tip inside cuvette. (b) The actual arrangement of axicon tip inside the cuvette at a depth >1 cm and the side-viewing objective. (c) TPE fluorescence of a trapped 3 μm polystyrene particle at laser beam power of 84 mW, as visible to the naked eye. (d) Bright field image of trapping along with TPF. (e) TPF from the trapped particle with IR cut-off filter. (f) Zoomed image of trapped and two-photon excited fluorescent particle with IR filter. (g) Bright field image of two trapped particles along axial direction with TPF. (h) TPF from the trapped particles with IR cut-off filter. (i) Zoomed image of trapped and two-photon excited fluorescent particles with IR filter. (j) TPF intensity as a function of average power of the fs laser beam and the fitted curve using a quadratic equation.

4 Results and Discussion

4.1 *Trapping and TPE of Fluorescent Objects Using Axicon Tip Single Optical Fiber*

Theoretical simulation of forces exerted by the beam from the microaxicon tipped single fiber on dielectric objects showed that the axial gradient force can overcome the scattering force even for nanoobjects, thus enabling single beam three-dimensional trapping using fiber-optic axicon with 20 deg $< \theta <$ 40 deg. Though fs tweezing was as effective as cw tweezing, the Ti:Sapphire laser was operated in fs mode only for the time period for TPF recording, so as to cause least damage[2] to the trapped sample. Figure 5 shows two-photon fluorescence excitation [Fig. 5(b)] while trapping fluorescent polystyrene particle [Fig. 5(c)] in a single fiber fs optical tweezers was realized using an axicon tip with $\theta = 20$ deg [Fig. 5(a)]. Quite stable two-photon excited fluorescence intensity was observed over the extended observation period (>5 min), under an inverted microscope. As discussed earlier, an intermediate axicon cone angle was found to provide better trapping stability. The two-photon fluorescence intensity map inside the particle was found to have a peak at an axial distance of 3.5 μm. However, the simulations showed that the beam waist is smallest at a distance of ~3 μm from the tip of the axicon for $\theta = 20$ deg. The small deviation from the simulated beam profile can be attributed to the presence of the particle acting as a microlens and refocusing the laser beam.

It may be noted that in contrast to two-photon excitation using a high NA microscope objective, a relatively longer streak of fluorescence was observed along the microsphere length [Fig. 5(c)] for microaxicon-based excitation. For $\theta = 20$ deg, the propagation distance was theoretically estimated to be ~4 μm, which matched the observed fluorescence. This has a distinct advantage for high signal-to-noise ratio detection of cells and molecules in the trapped region. However, this compromises the axial resolution. For higher axial resolution, smaller cone angle microaxicon may be used. Indeed near-field trapping can be achieved[14] using very small cone angle fiber axicons and therefore it can achieve two-photon excitation with high depth resolution.

4.2 *In-Depth Trapping and Two Photon Excitation of Trapped Fluorescent Microscopic Objects*

Figure 6 shows trapping and two photon excitation of trapped fluorescent microspheres at depth exceeding few cm. The axicon tip [Fig. 6(a)] was immersed in the fluorescent microsphere suspension as shown in Fig. 6(b). The side-viewing objective (10×, NA = 0.25) was used to image the tip and the trapped fluorescent particles inside the cuvette at a depth >1 cm [Fig. 6(b)]. Figure 6(c) shows the image of TPE fluorescence from a trapped 3 μm polystyrene particle at laser beam power of 84 mW in mode-locked condition. The highly-localized TPF was clearly visible to the naked eye. Figure 6(d) (Video 1) shows bright field image of trapping of the particle along with TPF using the side-viewing objective. With use of an IR cut-off filter, the TPF from the trapped particle could be filtered from the scattered light [Fig. 6(e)]. Figure 6(f) shows a zoomed view of the trapped and two-photon excited fluorescent particle. The bright field image of two particles trapped along the axial direction is shown in Fig. 6(g). Figure 6(h) shows the TPF from both the trapped particles. The axial positioning of the two particles will be influenced by the propagation distance of the Bessel–Gauss beam and also by mutual interaction due to optical binding.[14] Further, axial optical binding is known to depend on the size of the particle and therefore it will influence the distance between the two particles. Owing to the fact the these events occurred at a large depth from all sides of the cuvette, the side viewing objective with low NA limited us from resolving the distance between the two optically bound particles.

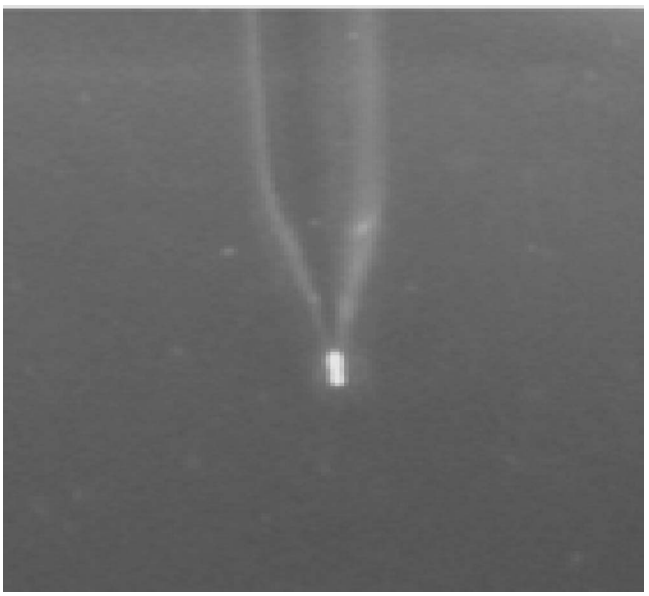

Video 1 Two-photon fluorescence from particles, trapped fiber optically inside a cuvette at a depth of centimeters. (QuickTime, 236 KB) [http://dx.doi.org/10.1117/1.3643340.1]

The fiber optic trapping was so stable that the TPF was observed by naked eye when holding the fiber in hand. Further, the trapped particle could be moved in 3D by slow maneuvering of the fiber. Figure 6(i) shows a zoomed view of the trapped and two-photon excited fluorescent particles with IR filter. The fact that a similar level of TPF intensity was observed from both the trapped particles indicates that the particle near the axicon tip might have refocused the laser beam onto the second particle [Fig. 6(i)]. Figure 6(j) shows variation of the TPF intensity from the trapped particle as a function of average power of the fs laser beam. Fitting the data to a quadratic equation showed a two-photon nature of the process.

It may be noted that a significantly large observation time could be achieved due to reduced photobleaching in the case of TPF excitation. The combination of the two noncontact methods in a single assay offers a powerful tool for studying cellular systems in large depths not possible earlier, by allowing simultaneous correlations made between molecular changes reported by fiber optic TPF, and micromechanical transitions probed by the fiber optical tweezers. The combined use of TPE and optical trapping using a single fiber optical device will enable in-depth analysis of nonadherent samples in microfluidic as well as bulk samples for *in situ* diagnostics. With the help of a 2×1 fiber optic splitter, the axicon-tip fiber, used for trapping, can collect the two-photon excited fluorescence (instead of the side-viewing imaging CCD used in the present study) for further analysis. Illustration of the concept for highly-sensitive detection of fluorescently-stained bacteria by two-photon excitation

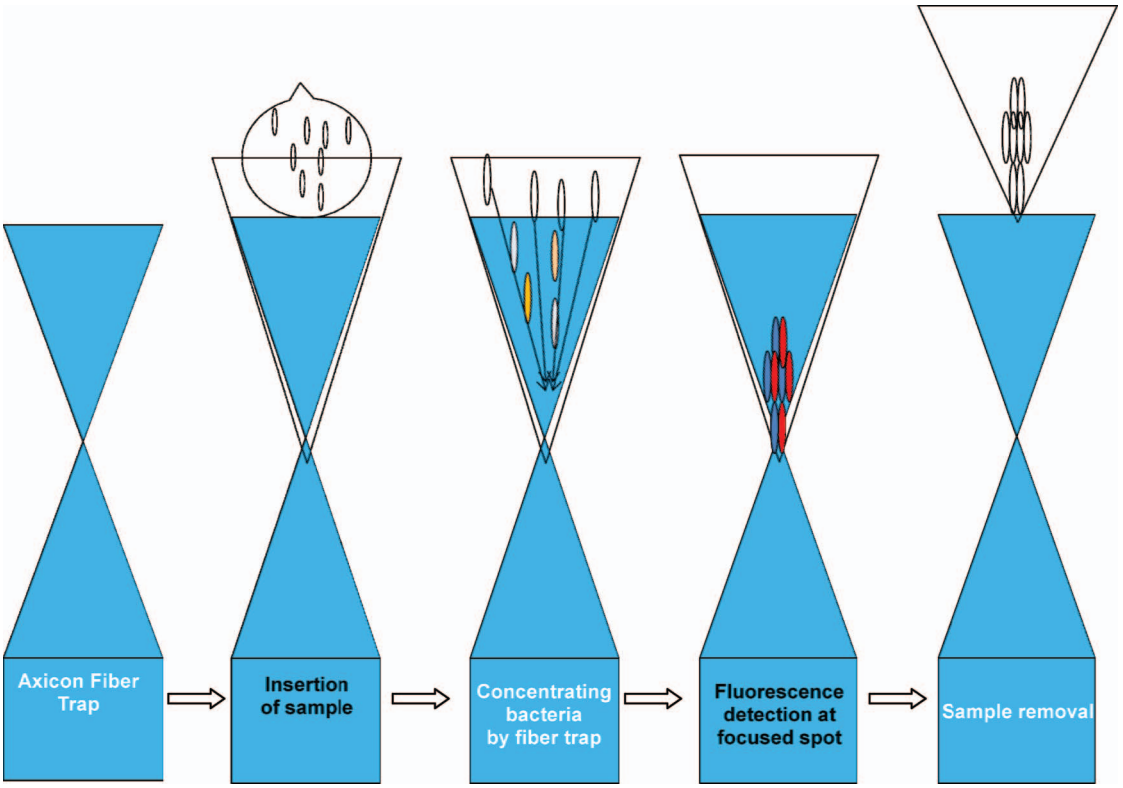

Fig. 7 Illustration of the concept for highly-sensitive detection of fluorescently-stained bacteria by two-photon excitation subsequent to concentration of the bacteria using fiber optic tweezers.

subsequent to concentration of the bacteria using fiber optic tweezers is shown in Fig. 7.

5 Conclusions

Theoretical simulations and experiments on the use of an axicon-tipped single fiber probe for simultaneous trapping and TPE fluorescence of fluorescent nano/microscopic particles were demonstrated. The axial confinement of TPE and trapping efficiency was found to be dependent on the cone angle of the fiber tips owing to the increasing propagation distance of the Bessel-like beam with increasing tip cone angle. Using this method, trapping depth of a few centimeters was achieved inside the colloidal sample with TPF from the trapped object(s) being visible to the naked eye. The integrated fiber optic manipulation and spectroscopy/imaging modality will enable *in situ* diagnosis of diseases at cellular level and help understand the cause of physical and biochemical changes during progression of a disease. Along with in-depth trapping and excitation of fluorophores, the proposed microaxicon tipped optical fiber can also be used for rotation, stretching, and ablation of microscopic samples.

Acknowledgments

The authors would like to thank M. Pinto for help in preparation of the manuscript.

References

1. A. Ashkin, J. M. Dziezic, J. E. Bjorkholm, and S. Chu, "Observation of a single beam gradient force optical trap for dielectric particles," *Opt. Lett.* **11**, 288–290 (1986).
2. Y. Liu, G. J. Sonek, M. W. Berns, and B. J. Tromberg, "Physiological monitoring of optically trapped cells: assessing the effects of confinement by 1064-nm laser tweezers using microfluorometry," *Biophys. J.* **71**(4), 2158–2167 (1996).
3. C. M. Creely, G. Volpe, G. P. Singh, M. Soler, and D. V. Petrov, "Raman imaging of floating cells," *Opt. Express* **12**, 6105–6110 (2005).
4. S. W. Hell, M. Booth, and S. Wilms, "Two-photon near- and far-field fluorescence microscopy with continuous wave excitation," *Opt. Lett.* **23**(15), 1238–1240 (1998).
5. E.-L. Florin, A. Pralle, J. K. H. Horber, and H. K. Stelzer, "Photonic force microscope based on optical tweezers and two-photon excitation for biological applications," *J. Struct. Biol.* **119**, 202–211 (1997).
6. W. Denk, J. H. Strickler, and W. Webb, "Two-photon laser scanning fluorescence microscopy," *Science* **248**, 73–76 (1990).
7. M. Goksor, J. Enger, and D. Hanstorp, "Optical manipulation in combination with multiphoton microscopy for single-cell studies," *Appl. Opt.* **43**, 4831–4837 (2004).
8. Y. Tanaka, H. Yoshikawa, and H. Masuhara, "Two-photon fluorescence spectroscopy of individually trapped pseudoisocyanine j-aggregates in aqueous solution," *J. Phys. Chem. B* **110**, 17906–17911 (2006).
9. B. Agate, C. Brown, W. Sibbett, and K. Dholakia, "Femtosecond optical tweezers for in-situ control of two-photon fluorescence," *Opt. Express* **12**, 3011–3017 (2004).
10. E. Sidick, S. D. Collins, and A. Knoesen, "Trapping forces in a multiple-beam fiber-optic trap," *Appl. Opt.* **36**(25), 6423–33 (1997).
11. K. Taguchi and N. Watanabe, "Single-beam optical fiber trap," *J. Phys. Conf. Ser.* **61**, 1137–1141 (2007).
12. K. S. Mohanty, C. Liberale, S. K. Mohanty, and V. Degiorgio, "In depth fiber optic trapping of low-index microscopic objects," *Appl. Phys. Lett.* **92**, 151113 (2008).
13. S. K. Mohanty, K. S. Mohanty, and M. W. Berns, "Manipulation of mammalian cells using single-fiber optical microbeam," *J. Biomed. Opt.* **13**, 054049 (2008).
14. S. K. Mohanty, K. S. Mohanty, and M. W. Berns, "Organization of microscale objects using a microfabricated optical fiber tip," *Opt. Lett.* **33**, 2155–2157 (2008).

15. S. K. Eah, W. Jhe, and Y. Arakawa, "Nearly diffraction-limited focusing of a fiber axicon microlens," *Rev. Sci. Instrum.* **74**, 4969–4971 (2003).
16. P. Hoffmann, B. Dutoit, and R. P. Salathe, "Comparison of mechanically drawn and protection layer chemically etched optical fiber tips," *Ultramicr.* **61**, 165–170 (1995).
17. Y.-H. Chuang, K.-G. Sun, C.-J. Wang, J. Y. Huang, and C.-L. Pan, "A simple chemical etching technique for reproducible fabrication of robust scanning near-field fiber probes," *Rev. Sci. Instrum.* **69**, 437–439 (1998).
18. J. W. Goodman, *Introduction to Fourier Optics*, Mc-Graw Hill, New York (1968).
19. Y. Harada and T. Asakura, "Radiation forces on a dielectric sphere in the Rayleigh scattering regime," *Opt. Comm.* **124**, 529–541 (1996).